Inorganic Chemistry

Article

pubs.acs.org/IC

Fluorinated Hydrotalcites: The Addition of Highly Electronegative Species in Layered Double Hydroxides To Tune Basicity

Enrique Lima,*[,†] María de Jesús Martínez-Ortiz,[‡] Renata Isabel Gutiérrez Reyes,[‡] and Marco Vera[§]

[†]Instituto de Investigaciones en Materiales, Universidad Nacional Autónoma de México, Circuito exterior s/n, Cd. Universitaria, Del. Coyoacán, CP 04510, México D. F., Mexico

[‡]Instituto Politécnico Nacional—ESIQIE, Avenida IPN UPALM Edificio 7, Zacatenco, 07738 México D.F., Mexico

[§]Universidad Autónoma Metropolitana, Iztapalapa, Av. San Rafael Atlixco No. 186, Col. Vicentina, CP 09340, México D.F., Mexico

ABSTRACT: Hydrotalcite-like compounds were synthesized by coprecipitation using a constant-pH method. Aluminum was introduced in the form of an octahedral aluminum fluorine complex during the synthesis. Controlling the pH during the synthesis ensured that aluminum fluorine did not decompose to tetrahedral species but remained in the octahedral $(AlF_6)^{3-}$ form to be incorporated into brucite-like sheets. The physicochemical, thermal, and spectroscopic characterizations showed significant modifications by fluorine introduction regarding structural, textural, and adsorption properties. The memory effect of fluorinated hydrotalcites differed from the memory effect commonly observed in fluorine-free hydrotalcites. Nitromethane adsorption showed that the basicity of hydrotalcite was greatly modified by the fluorine loading.

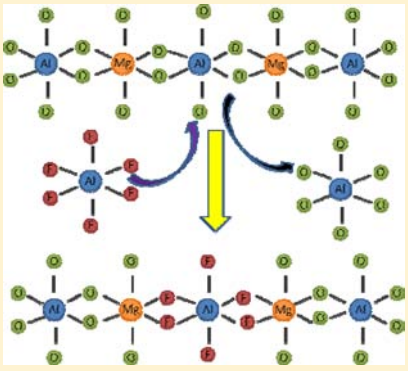

INTRODUCTION

Layered double hydroxides (LDHs), commonly called hydrotalcite-like compounds (HTs), are a broad family of compounds with acid−base properties.[1−3] They are used in important applications in the form of catalysts, catalyst supports, adsorbents, and ionic exchangers.[4−6] For instance, these solids are capable of performing intercalation reactions, thus providing an excellent tool to explore the parameters that affect the reactivity of intercalated species by modifying their immediate environment and by imposing on these species a two-dimensional constrained system.

The structure of LDHs can be derived from a brucite structure $(Mg(OH)_2)$, which is composed of linked octahedrons of magnesium hydroxide. The octahedrons form gibbsite-type sheets stacked in a hexagonal space group.[7] In LDHs, a fraction of the divalent Mg^{2+} ions is substituted by trivalent cations, e.g., Al^{3+}. Because of this substitution, the hydroxide layers become positively charged but are charge-compensated by interlayer anions or anionic complexes. LDHs can form in a broad range of compositions, described by the formula $[M^{2+}_{1-x}M^{3+}_x(OH)_2][A^{n-}]_{x/n}\cdot mH_2O$, where M^{2+} and M^{3+} are the di- and trivalent cations in the octahedral positions within the hydroxide layers. The value of x commonly ranges from 0.17 to 0.33. A^{n-} represents an exchangeable interlayer anion that can vary. Although carbonate anions have the largest affinity, large anionic species can also intercalate into the space between the layers.[8−10] The M^{3+} ion often is Al^{3+} but may also be one of a number of trivalent cations, including those of Ga, Cr, and Fe. Similarly, the M^{2+} ion is not specific to Mg^{2+}; M^{2+} can also be Ni^{2+}, Zn^{2+}, Cu^{2+}, or another divalent cation. These ions can be incorporated to brucite-like layers.

The layered structure collapses due to dehydration, dehydroxylation, and anion loss when LDH is treated at temperatures between 200 and 400 °C. When this collapse occurs, mixed oxides are often obtained, which are commonly able to recover the layered structure when put in contact with water or an anionic aqueous solution. The collapse-recovery of the layered structure is frequently referred to as the "memory effect".[11−13] During calcination, the coordination of M^{3+} ions is partially lowered from octahedral to tetrahedral.[14,15] Moreover, in the rehydration step, some of the tetrahedral M^{3+} ions do not recover this octahedral coordination.[16,17] Therefore, the physicochemical properties of the reconstructed structure become different from those of the original LDH. This process is an approach to modify the physicochemistry of these LDHs solids.

Chemical composition variation continues to be the best strategy to tune the acid−base properties of LDHs. In the LDH structure, the M^{3+} cations occupy octahedral positions, surrounded by six oxygen atoms (of the OH^- anions) as first neighbors. However, to date, no anion other than hydroxyl has been tested for incorporation into the brucite-like sheets. It is likely that other anions are also suitable to tune and diversify the types of acid−base pairs available. Thus, the goal of this study was to introduce anions other than oxygen into the octahedral layers. In this paper, we report for the first time the preparation of hydrotalcite with partial substitution of the $(Al(OH)_6)^{3-}$ octahedra by $(AlF_6)^{3-}$, with the understanding that

Received: April 18, 2012
Published: June 29, 2012

   dx.doi.org/10.1021/ic300799e | *Inorg. Chem.* 2012, 51, 7774−7781

the introduction of highly electronegative fluorine changes the capacity of LDH to attract polarized and polarizable species.

The fluorination of LDH was previously reported, where fluoride anions were incorporated between the brucite-like layers.[18−20] The fluorides, as compensating anions, are labile species, and it is expected that eventually fluorides are exchanged but other selective anions such as carbonates. The incorporation of fluorine as a part of the brucite-like layers, substituting the OH structural groups, has not been explored.

EXPERIMENTAL PROCEDURE

Materials. Carbonate-containing Mg−Al LDHs with a Mg/Al atomic ratio close to 3 were prepared by coprecipitation at pH 10. An aqueous solution containing appropriate amounts of $Mg(NO_3)_2{\cdot}6H_2O$, $Al(NO_3)_3{\cdot}6H_2O$, and Na_3AlF_6 (Aldrich, 99.99%) was delivered into a reactor by a chromatographic pump at a constant flow of 1 cm^3/min. A second aqueous solution containing 2.0 M solution of NaOH (Aldrich, 99%) was simultaneously fed. The pH remained constant by controlling the addition of the alkaline solution using a pH-STAT Titrando apparatus (Metrohm, Switzerland). The suspension was stirred overnight at 80 °C, and then the solid was separated by centrifugation, rinsed thoroughly with distilled water, and dried overnight at 80 °C. The ratio of Mg/Al was maintained at 3 in the samples reported in this work. The source of aluminum was either aluminum nitrate or a mixture of aluminum nitrate with sodium hexafluoro-aluminate.

Memory Effect. The LDH samples were thermally decomposed by heating to 450 °C (heating rate: 3 °C/min) for 3 h. Heat treatment caused the formation of periclase-like (Mg,Al)-oxide solutions that recovered the layered structure upon exposure to water vapor.

Characterization. The samples were characterized by X-ray diffraction (XRD), nuclear magnetic resonance (MAS NMR) of ^{27}Al and ^{19}F nuclei, thermal analysis (TGA), infrared spectroscopy (FTIR-ATR), N_2 adsorption, and nitromethane adsorption followed by ^{13}C MAS NMR.

The XRD patterns were acquired using a diffractometer D8 Advance-Bruker equipped with a copper anode X-ray tube. The presence of pure LDH (native sample) and periclase (sample thermally activated) structures was confirmed by fitting the diffraction patterns with the corresponding Joint Committee Powder Diffraction Standards (JCPDS cards).

Infrared spectra were recorded using a Perkin-Elmer series spectrophotometer model 6X operated in the ATR-FTIR mode with a resolution of 2 cm^{-1}.

The single pulse solid-state ^{27}Al and ^{19}F MAS NMR single excitation spectra were acquired on a Bruker Avance 300 spectrometer. The single pulse ^{27}Al NMR spectra were acquired under MAS conditions by using a Bruker MAS probe with a cylindrical 4 mm o.d. zirconia rotor and by operating the spectrometer at a frequency of 78.1 MHz. Short single pulses ($\pi/12$) were used. The 90° solid pulse width was 2 μs, and the chemical shifts were referenced to those of an aqueous 1 M $AlCl_3$ solution. The MAS frequency was 10 kHz. All the NMR measurements were done at room temperature (19 °C).

The ^{19}F MAS NMR spectra were measured by operating the spectrometer at 376.3 MHz, using $\pi/2$ pulses of 6 ms with a recycle delay of 1 s; ^{19}F chemical shifts were referenced to those of $CFCl_3$ at 0 ppm.

The nitrogen adsorption−desorption isotherms were determined with Bel-Japan Minisorp II equipment, using a multipoint technique. The samples were previously calcined at 450 °C for 3 h and then evacuated under a vacuum for 10 h. Surface areas were calculated with the BET equation, and pore diameter values were calculated using the BJH method.

NH_3 TPD measurements were performed in a microreactor assembly where 250 mg of solid was treated at 450 °C for 3 h and then cooled prior to NH_3 adsorption. The sample was in contact with 30 mL/min of NH_3 for 50 min, and then was flushed with N_2 at 100 °C for 60 min. The desorption profile was recorded with a heating rate of 10 °C/min in the range 80−500 °C using a GC equipped with a TCD detector.

Thermogravimetric analyses were performed with TA Instruments equipment. The samples were heated at a rate of 5 °C min^{-1} from room temperature to 900 °C in a nitrogen atmosphere.

Nitromethane Adsorption. Batches of approximately 100 mg of the samples were packed in a glass cell equipped with a resealable valve that was suited for attachment to a vacuum line. The batches were then evacuated for 10 h at 450 °C. The samples were equilibrated with 30.0 Torr of $^{13}CH_3NO_2$ at room temperature for 30 min and then desorbed at 50 °C for 30 min. The powder was then packed into 4 mm NMR rotors under an inert (argon) atmosphere. The ^{13}C CP/MAS NMR spectra were acquired at room temperature using a Bruker Avance 400 spectrometer operating at the Larmor frequency of 100.5 MHz, with a contact time of 5 ms, a spinning rate 5 kHz, and $\pi/2$ pulses of 5 μs. Chemical shifts were referenced to those of the CH_2 groups of solid adamantane at 38.2 ppm relative to TMS.

RESULTS AND DISCUSSION

Fresh and Thermally Treated Samples. The XRD patterns of the fresh and thermally treated LDH samples are shown in Figure 1. The diffractogram of the fresh samples, as

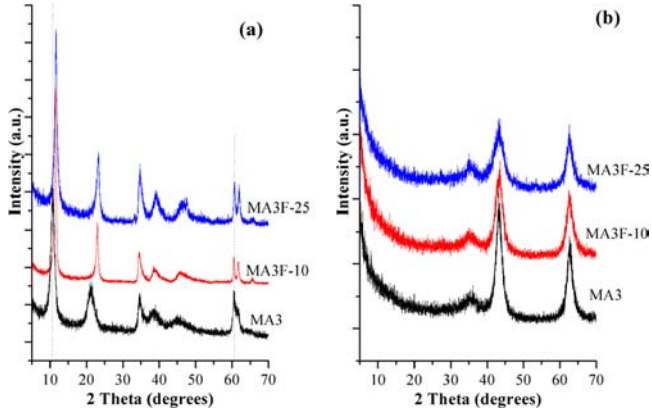

Figure 1. X-ray diffraction patterns of LDH as synthesized (a) and after thermal treatment at 550 °C (b). Dotted line in part a was included as a guide to evidence the slight shift of the (003) plane at 10.5° taken as a reference for the plane (110) at 60.4°.

shown in Figure 1a, matched that of hydrotalcite (JCPDS card 22-0700), regardless of the presence or absence of fluorine. This result is evidence that no crystalline fluorine compounds were segregated at the surface of LDH. Moreover, the position of the XRD peak attributed to the (003) plane was aligned with that of a carbonated hydrotalcite,[21] although the position of the peak varied slightly with fluorine content. Increasing the amount of fluorine resulted in a higher diffraction angle, which suggests that, with increasing fluorine species, the attraction between the anions and the brucite-like layer is stronger in such a way that the distance between the layers diminished, Table 1. This is not surprising because fluorine is able to form strong hydrogen bonds[22] with hydrogen atoms from water to influence the crystal-growth step, as evident in the narrower XRD peaks of the fluorinated samples. Upon thermal treatment, the layered structure disappeared, giving way to the periclase-like structure (Figure 1b). In the case of the MA3 sample, the composition corresponded to that of a mixed oxide of Mg(Al)O, but in the case of MA3F-10 and MA3F-25, their mixed oxides were fluorinated. The presence of fluorine in the mixed oxides was not evident in the XRD characterization. In this respect, the NMR results in Figure 2 are more illustrative.

dx.doi.org/10.1021/ic300799e | Inorg. Chem. 2012, 51, 7774−7781

Table 1. Characteristics of Fluorinated LDH Samples Synthesized by Coprecipitation Method

code sample	chemical formula[a]	Mg/Al ratio	d_{003} (Å)[b]	BET area (m^2/g)	av pore radius[c] (nm)
MA3	$[Mg_{0.761}Al_{0.248}(OH)_2](CO_3)_{0.124}0.66H_2O$	3.06	24.92	190	10.7
MA3F-10	$[Mg_{0.752}Al_{0.253}(OH)_{1.93}F_{0.07}](CO_3)_{0.126}0.58H_2O$	2.98	23.17	174	13.8
MA3F-25	$[Mg_{0.738}Al_{0.242}(OH)_{1.73}F_{0.27}](CO_3)_{0.121}0.58H_2O$	3.04	22.76	137	12.24

[a]As determined by chemical analysis. [b]Calculated from XRD pattern. [c]Determined by N_2 isotherms and BJH method.

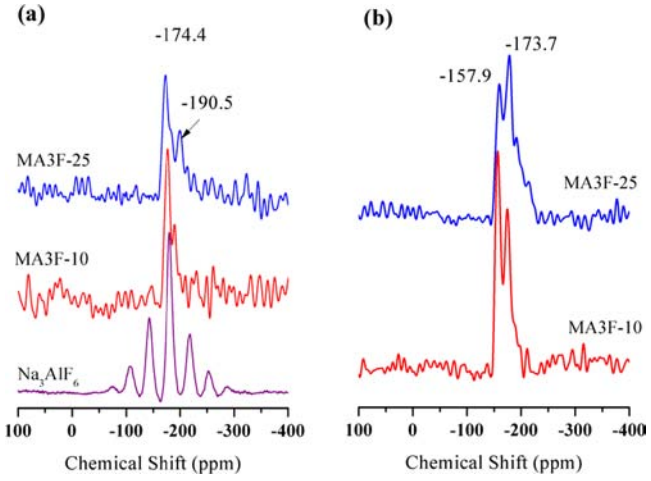

Figure 2. ^{19}F MAS NMR spectra of fresh samples (a) and after thermal treatment at 550 °C (b).

Figure 2a shows the ^{19}F MAS NMR spectra of the fresh samples. Regardless of the amount of fluorine that was incorporated, two peaks continued to be observed. The first peak at −174.4 ppm corresponds to Na_3AlF_6, whose spectrum was also included in Figure 2a for reference. Therefore, the intense peak at −174.4 ppm is due to the AlF_6 octahedra, as has also been reported for other compounds,[23−25] e.g., MgF_6 and GaF_3-doped with MgF_2. Here, it has to be mentioned that the stability of $(AlF_6)^{3-}$ species in solution has been a subject of study.[26−28] The ionic equilibrium between $(AlF_6)^{3-}$ and $(AlF_4)^-$ in aqueous aluminum−sodium fluoride mixtures inclines to stabilize low-order complexes, e.g., $(AlF_4)^-$ and $(AlF_5)^{2-}$. It is also suggested that $(AlF_6)^{3-}$ species are also present in solution but in a lower amount. Furthermore, it is also reported that $(AlF_6)^{3-}$ is stabilized in liquid state by ionic screening interactions. Therefore, the synthesis of LDH in the presence of $(AlF_6)^{3-}$ is possible under alkaline conditions as those used in a coprecipitation synthesis, where $(AlF_6)^{3-}$ reacts to be incorporated to LDH, but in order to accomplish the Le-Chatelier's principle,[29] they are produced continuously during the synthesis.

In the spectra of fluorinated LDHs, a second NMR peak at −190.5 ppm suggests a second type of fluorine coordination, which was expected because the network anion consisted not only of F^- but also of OH^-. Actually, the inclusion of $(AlF_6)^{3-}$ into the brucite-like layers occurs most probably randomly, which implies that the first coordination sphere of fluorine contains both Al^{3+} and Mg^{2+} cations; therefore, FMg_5 and FMg_4 environments should be present, and the δ-values are consistent with those observed by Scholtz et al.[30]

^{19}F NMR spectra of the mixed oxides, which are displayed in Figure 2b, also show two narrow peaks but are shifted to weaker fields. This shift suggests that the order of the fluorine coordination was maintained even after the collapse of the layered structure, although the nature of the fluorine species was modified. This result is not surprising because the mixed $AlF_{6-x}O_x$ species is expected to appear upon structure collapse. As shown above, the ^{19}F NMR signal for AlF_6 appears at −190 ppm, but that of AlO_5F was reported[31] to be at −120 ppm, i.e., the larger the chemical shift the higher the number of oxygen atoms replacing fluorine in the aluminum octahedral. Thus, it can be concluded that, with thermal treatment, the LDH structure collapse was accompanied by the formation of mixed $AlF_{6-x}O_x$ species, which suggests that fluorine was redistributed. In line with this conclusion, one can see that, with increasing fluorine content, the NMR signal at weaker fields also increases, and the appearance of additional peaks, not well resolved, is observed.

The ^{27}Al MAS NMR results are also very useful to show important changes in LDH after fluorine incorporation. First, the isotropic NMR peak at 8.9 ppm showed that aluminum was 6-fold coordinated in all three fresh samples (Figure 3a). The

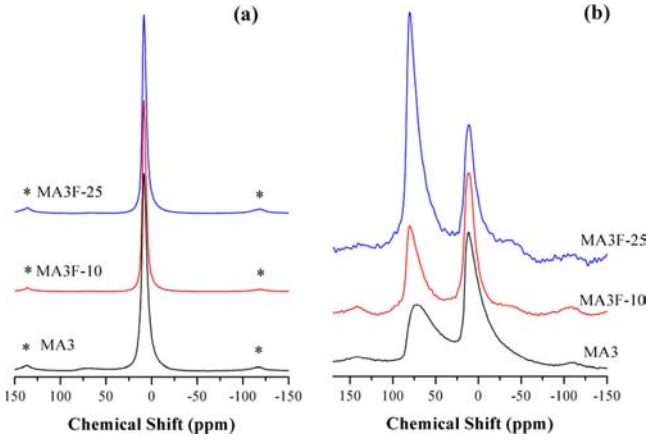

Figure 3. ^{27}Al MAS NMR spectra of fresh samples (a) and after thermal treatment at 550 °C (b). * indicates spinning side bands (10 kHz).

spectrum of $(AlF_6)^{3-}$ was also acquired as a reference (spectrum not shown). The isotropic peak was also located at 9 ppm, confirming that chemical shifts of $(Al(OH)_6)^{3-}$ and $(AlF_6)^{3-}$ are approximately the same. It should be noted, however, that the NMR peak is narrower for the fluorinated samples compared to the fluorine-free sample. This difference could be explained because F^- anions have substituted a part of OH^- groups that contain a polar covalent O−H bond, which leads to a diminution of dipolar interactions. Furthermore, it should be emphasized that ^{27}Al is a quadrupular nucleus ($I = {}^5/_2$); therefore, the ^{27}Al NMR spectrum in Figure 3 (acquired at 7 T) does not resolve, if any, the presence of $AlF_4(OH_2)$ or $AlF_3(OH)_3$. The existence of these species was previously reported, but it was necessary to acquire the ^{27}Al NMR spectra in a very high magnetic field strength (17.6 T).[32] With temperature, mixed oxides emerged as mentioned above, and the lowered coordination of aluminum became clear. In the spectra displayed in Figure 3b, the two peaks of ^{27}Al MAS

dx.doi.org/10.1021/ic300799e | Inorg. Chem. 2012, 51, 7774−7781

NMR that are characteristic of thermally treated LDH appeared at approximately 11 ppm (octahedral, Al(octa)) and 70−82 ppm (tetrahedral, Al(tetra)).[33,34] While the peak due to octahedral species appears at 11 ppm for three mixed oxide samples, the position of the tetrahedral peak is a function of the presence of fluorine. The NMR peak of the fluorine-free sample is observed at 69 ppm, while that corresponding to the fluorinated samples is at 82 ppm, due to the shielding effect of tetrahedral species by fluorine. Furthermore, the fluorinated samples had narrower peaks than the fluorine-free sample, which can be interpreted as an averaging of some dipolar effects in the fluorinated samples. Furthermore, the addition of fluorine has a strong effect on the relative intensities of resonances Al(tetra) and Al(octa). The ratio of their intensities (Al(tetra)/Al(octa)), as determined by the deconvolution and integration of spectra, are 0.62, 0.73, and 1.21 for MA3, MA3F-10, and MA3F-25, respectively. This result is relevant because Al(tetra) species are considered to be coordinatively unsaturated sites (CUS) of aluminum that can play the role of acid sites.[35,36] The results show for the first time that a mixed oxide, resulting from the calcinations of a LDH, has relative intensities with an Al(tetra)/Al(octa) ratio higher than 1, in contrast to prior reports demonstrating ratios between 0.5 and 0.7.[37] In acide-base catalysis, e.g., in some condensation reactions, these CUS sites are claimed to stabilize, partially, the anions produced by the base sites in order to react at surface.

A high number of CUS sites, of course, favors an increase in the solid acidity. In this respect, in Table 2 are reported the

Table 2. NH_3 Adsorbed on LDH Samples As Determined from TPD Measurements[a]

	NH_3 uptake (mmol/m^2) × 10^3			
sample	I	II	III	total
MA3	0.40	1.11	0.65	2.16
MA3F-10	0.66	2.72	0.60	3.98
MA3F-25	0.81	5.49	1.83	8.13

[a]I in the 200−300°C range, II in the 300−400°C range, and III in the 400-500°C range.

NH_3 amounts adsorbed in the LDHs, as determined by TPD measurements; the values are done in mmol/m^2 in order to avoid the effect of variation of specific surface. NH_3 uptake showed the presence of acid sites of different strength as generally occur in LDH samples. Three different temperature ranges were identified in the TPD profiles: I from 200 to 300 °C, II from 300 to 400 °C, and III from 400 to 500 °C. As shown in Table 1, the various LDH samples differed in fluorine content. In Figure 4 the NH_3 adsorbed was plotted as a fraction of fluorine that has replaced hydroxyl groups. The total amount of NH_3, the amount of sites with moderate strength (range II), as well as the Al(tetra)/Al(octa) ratio show a relationship linear with the fluorine content, showing indisputably the acidity increase by the fluorine presence. This feature is discussed further in the section of nitromethane adsorption.

XRD and NMR results have shown significant changes as a consequence of the introduction of fluorine into LDH sheets. We focus now on the FTIR results. Figure 5 shows the spectra of layered samples in which the broad absorption band between 3700 and 3000 cm^{-1} due to the O−H stretching is observed, and at 1635 cm^{-1}, the band attributed to the bending deformation of molecular water is present. Additionally, the band attributed to the asymmetric stretching of C−O bonds in

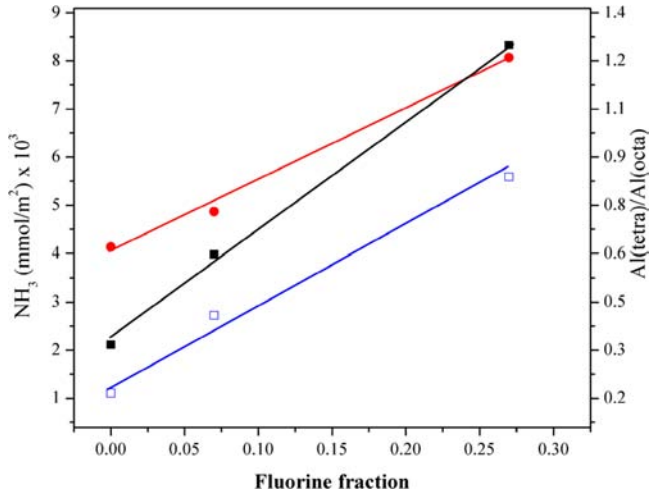

Figure 4. Amount of NH_3 adsorbed and Al(tetra)/Al(octa) in LDHs as a function of fluorine content: −■− total NH_3 adsorbed; −□− NH_3 measured from TPD in the 300−400 °C range; −●− Al(tetra)/Al(octa) ratio measured by integration of the corresponding ^{27}Al MAS NMR lines.

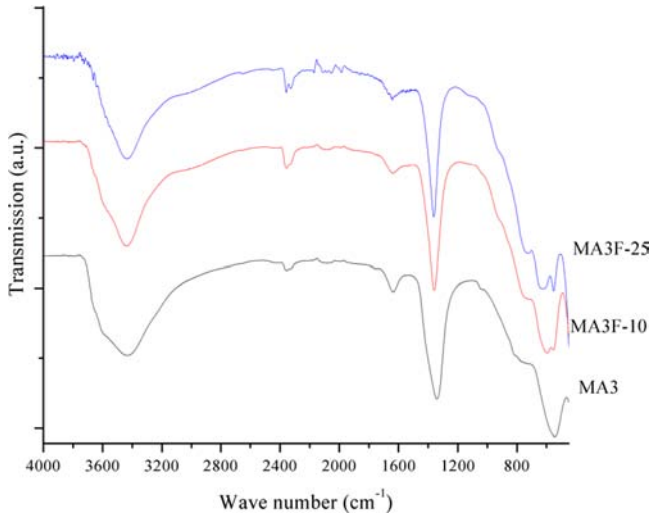

Figure 5. FTIR spectra of LDH samples.

carbonate ions[38,39] is observed between 1340 and 1360 cm^{-1}. Indeed the shape of this absorption band is affected by the composition of LDH; in the MA3 sample (noncontaining fluorine), an asymmetric band appears centered at 1340 cm^{-1}, while in samples MA3F-10 and MA3F-25, this band is symmetric and centered at 1350 and 1359 cm^{-1}, respectively. This result can be explained as the progressive decrease of vibration modes as a consequence of the fluorine incorporation. It seems that CO_3^{2-} anions are present in both C_{2v} and D_{3h} symmetry in MA3 sample, but they are mainly stabilized with symmetry D_{3h} in fluorine containing samples. The absorption bands due to translational mode metal−OH (δ-mode) were also dependent on the presence of fluorine; this band appears at 543, 590, and 631 cm^{-1} for MA3, MA3F-10, and MA3F-25, respectively. These results suggest that the interaction between carbonate anions and water is directly modified due to fluorine in the brucite-like layers, which strongly attracts water molecules. The absorption band due to symmetric stretching vibration of octahedral $(AlO_6)^{3-}$ species is observed at 540 cm^{-1} for both MA3F-10 and MA3F-25 samples. Lastly, infrared

dx.doi.org/10.1021/ic300799e | Inorg. Chem. 2012, 51, 7774−7781

integrated intensities of the broad OH stretching bands were measured by using the EZ OMNIC 32 software. The integrated intensities were 1249, 1138, and 994 for MA3, MA3F-10, and MA3F-2, respectively. These values provide, roughly, the percentage of OH groups substituted by fluorine to be 8.6 in MA3F-10 and 20.4 in MA3F-25 which does not necessarily match with the compositions of samples, Table 1. This difference was expected because the OH absorption band includes also the vibration modes of OH groups coming from H_2O and percentage of water varies in the samples. It should be emphasized that it seems that the OH species are selectively eroded upon fluorine incorporation. Actually, the OH absorption band is broader for the MA3 sample, suggesting that the OH lost are those with higher wave numbers, related to basic hydroxyls.

Figure 6 shows the thermal behavior of the MA3, MA3F-10, and MA3F-25 samples. It is clear that the fluorinated samples

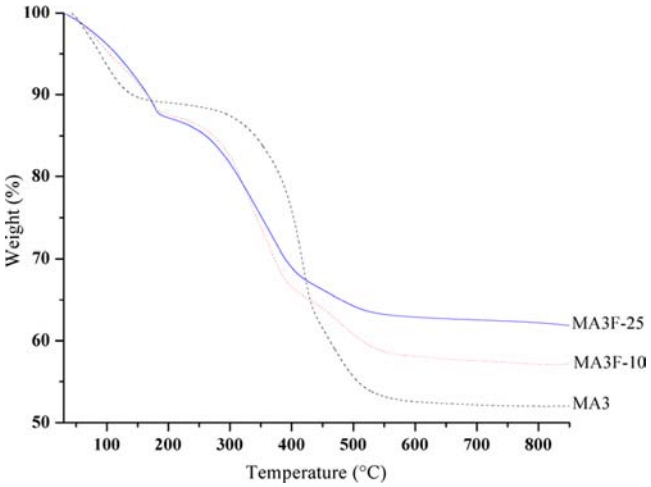

Figure 6. Thermogravimetric curves of the LDH samples in nitrogen.

behave differently from the fluorine-free sample. Initially, all three samples behaved similarly with respect to the initial loss of weight recorded between 40 and 170 °C, which corresponds to the loss of water from the superficial layers and the interlayer. Subsequently, the second loss of weight corresponds to decarbonation and dehydroxylation (200−500 °C), leading to the formation of the periclase structure. In this step, the presence of the fluorine clearly makes a difference: this step occurs at higher temperatures for the fluorinated samples, which is in agreement with stronger interaction of layers−anions as a consequence of the presence of fluorine, as suggested by FTIR and XRD. Further, the fluorine-free sample lost more weight than the fluorinated samples; specifically, sample MA3 lost 10% more weight than the MA3F-25 sample, which suggests that dehydroxylation occurred instead of defluorination. These results agree with our previous NMR characterizations, and it is expected that the changes concerning the hydration process modify the textural properties of LDH. Therefore, the nitrogen adsorption−desorption isotherms were measured.

The N_2 isotherms for the three samples, fitted with type IV, have a hysteresis of type III, according to IUPAC classification.[40] For the sake of brevity, a figure with the nitrogen isotherms was not included. The textural parameters that emerged from N_2 adsorption−desorption are reported in Table 1. The presence of fluorine modifies the properties of LDH, but the fluorine has a negative effect on the development of specific surface area. This result was expected because the thermal analyses have shown that the capacity of fluorinated samples to trap water differs from that of the free-fluorine-sample. Before the nitrogen adsorption measurements, the samples were activated at 450 °C for 3 h and then evacuated under vacuum. This treatment did not ensure that the three samples were completely eliminated of water and carbonates. The surface was not dramatically devoid of the presence of fluorine, which can be attributed to the increase in pore size, Table 1.

Memory Effect. The XRD patterns displayed in Figure 7 confirm that the lamellar structure of hydrotalcite was

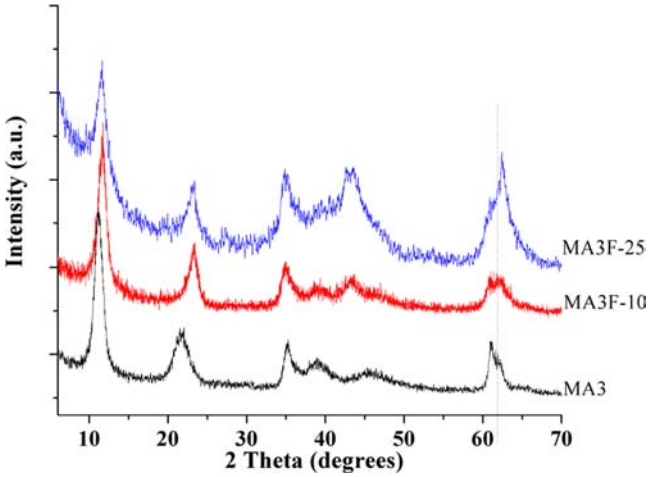

Figure 7. X-ray diffraction patterns of samples after a memory effect cycle. The thermal treatment was at 550 °C and the rehydration in a saturated (100%) water atmosphere.

recovered after the calcination−hydration cycle. No crystalline fluorine compounds were segregated at the surface of rehydrated LDH. Furthermore, the position of the XRD peak attributed to the (003) plane continued to be dependent on fluorine content. As observed and explained for the native samples, as the amount of fluorine increased, the diffraction angle also increased.

Figure 8 displays the ^{19}F MAS NMR spectra of the thermally treated MA3F-25 sample that was then rehydrated by exposing them to water vapor for variable periods. At very short rehydration times (2 h), the two peaks observed for mixed oxides, at −174.4 and −190.5 ppm, remained. However, for hydration times longer than 6 h, the peak at −174.4 ppm diminishes, but the peak at −190.5 ppm (after 2 h rehydration) shifted to higher chemical shifts values up to −169.9 ppm (after 6 h rehydration). This result suggests that, before rehydration, $AlF_{6-x}O_x$ species enriched in fluorine existed, presumably AlF_6 (NMR peak at −190.5) as well as $AlF_{6-x}O_x$ species enriched in oxygen (peak at −174.4). With hydration, the recovering of layered structure occurred, which was accompanied by a redistribution of fluorine. The appearance of a broad peak centered at −169 ppm is assumed to be due to a more homogeneous repartition of fluorine during the formation of the layers. These results agree with those presented in Figure 9 where the ^{27}Al MAS NMR spectra show that the coordination of aluminum progresses as a function of the hydration time. Upon the exposure of samples to water vapor for periods as short as 2 h, tetrahedral aluminum was generated in the thermal

dx.doi.org/10.1021/ic300799e | Inorg. Chem. 2012, 51, 7774−7781

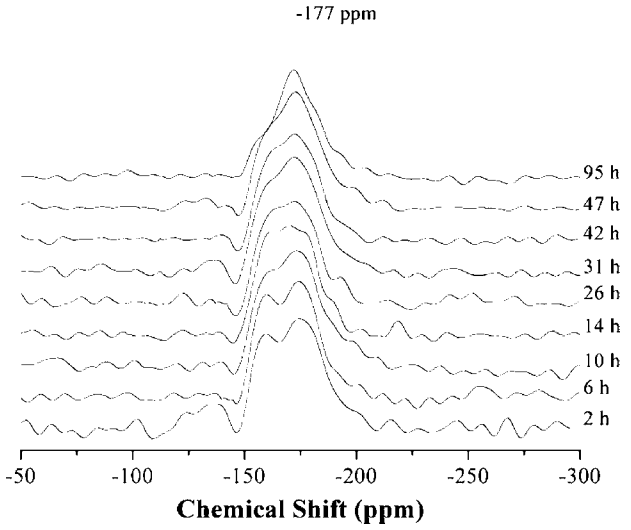

Figure 8. ^{19}F MAS NMR spectra of LDH MA3F-25 sample after thermal treatment at 550 °C and consequent rehydration.

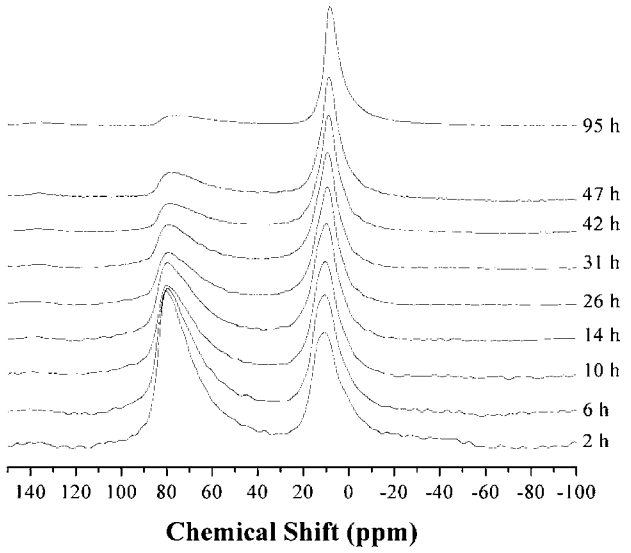

Figure 9. ^{27}Al MAS NMR spectra of LDH MA3F-25 sample after thermal treatment at 550 °C and consequent rehydration.

treatment step (Figure 3b) to partially recover the octahedral coordination. As the hydration time progresses, more tetrahedral aluminum is converted to Al(octa), consistent with the XRD results that showed the recovery of the layer structure. Note that the thermally treated sample contained a higher fraction of Al(tetra). At the end of rehydration, however, the spectrum of the native sample (Figure 3a) was not fully recovered, with a minor percentage of aluminum remaining in the Al(tetra) coordination. The width of NMR Al(octa) peak of the rehydrated MA3F-25 sample is 503 MHz, which has a value between the width of the corresponding peaks of native MA3 (619 MHz) and native MA3F-25 (397 MHz), confirming that the fluorine was redistributed more homogeneously in the sample after one memory-effect cycle. However, the MA3F-25 sample does not exhibit this property because although the XRD showed the layer structure reconstruction, the NMR results suggest the formation of CUS of aluminum instead. This result shows the importance of incorporation of fluorine forming part to the layers and no incorporated these species as fluorides by ionic exchange[41] or impregnation where eventually are easily removed.

Nitromethane Adsorption. Because of its polarizable NO_2 group, nitromethane was chosen as a probe molecule to be adsorbed onto the mixed oxides that emerged from the thermal treatment of the fluorinated samples. The ^{13}C CP/MAS NMR spectra of nitromethane adsorbed on Mg(Al)O and that of the fluorinated Mg(Al)O samples at room temperature followed by desorption of physisorbed species at 28 °C are shown in Figure 10. The isotropic peak at 107 ppm, in the spectrum of the

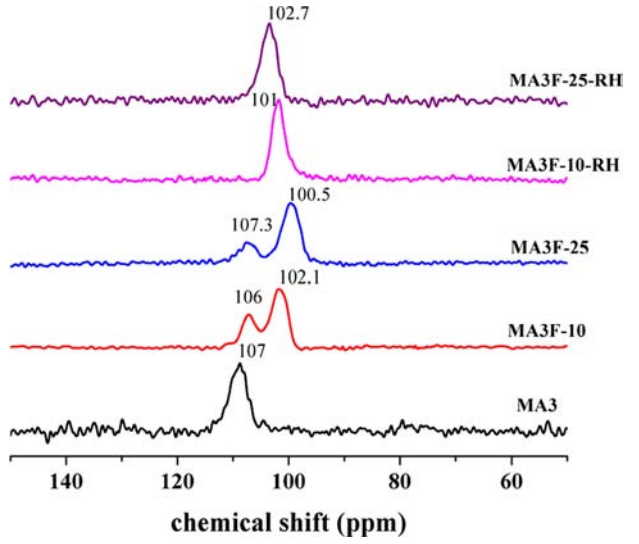

Figure 10. ^{13}C CP/MAS NMR spectra of nitromethane adsorbed on LDH samples. The prefix RH added to the name of two samples indicates that the native sample was thermal treated and then rehydrated. All samples, previous to nitromethane adsorption, were activated at 450 °C for 10 h under vacuum.

fluorine-free sample, is due to the methylene group of chemisorbed aci-anion nitromethane. These assignments are in accordance with those previously reported for nitromethane adsorbed onto MgO and mixed oxides Mg(Al)O.[42−44] In fluorinated samples, the peak of the methylene groups give two peaks in the 100−110 ppm range. It is worth noting that the chemical shift of the methylene group of the chemisorbed aci-anion nitromethane depends on the composition of the oxide. The adsorption of nitromethane on the MA3 sample leads to an upfield shift to 107 ppm. Conversely, the adsorption on the MA3F-10 and MA3F-25 samples leads to spectra consisting of a peak at 107 ppm and a second peak with a downfield shift (position at approximately 100 ppm). On the contrary, the fluorinated mixed oxides obtained from the thermal treated rehydrated LDH lead to spectra with a single signal due to methylene groups (101−102 ppm). These results agree with the assumption that a redistribution of fluorine occurs with the memory effect. Further, the two peaks within 100−107 ppm observed for the fluorinated mixed oxides from the MA3F-10 and MA3F-25 samples indicate that microdomains enriched in fluorine were present. To comprehend the variation of the observed ^{13}C isotropic chemical shift of chemisorbed anion of nitromethane, it is assumed that the solids possess enough basicity to extract a proton from the methyl group in nitromethane. The anion obtained interacts with the conjugate Lewis acid sites of the mixed oxide surface, leading to an electron shift from the double bond, Scheme 1. The isotropic

dx.doi.org/10.1021/ic300799e | Inorg. Chem. 2012, 51, 7774−7781

Scheme 1

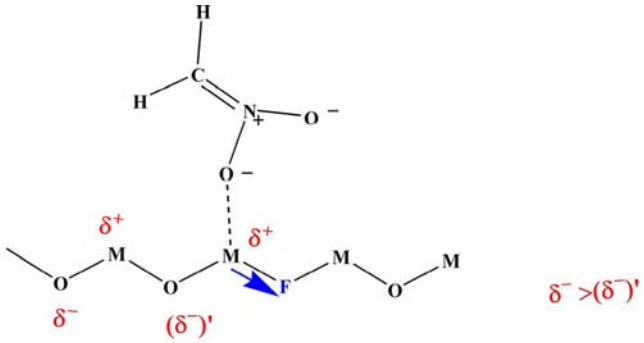

downfield shift of the methylene for the adsorbed anion of nitromethane can be attributed to a strong interaction between the conjugate Lewis acid site and the adsorbed molecule. Therefore, the NMR shift reflects the strength of the Lewis sites of the conjugate base sites because increasing Lewis acidity strength corresponds to the lowering of the basic strength. Thus, it can be concluded that the presence of fluorine in the surface induces the formation of strong basic sites at the surface of fluorinated mixed oxides, as shown in Scheme 1.

CONCLUSION

Fluorine was successfully incorporated to the hydrotalcite-like compounds. Fluoride anions take the position of hydroxyl anions, thus modifying the textural, structural, adsorption, and thermal properties of the layered double hydroxide. With thermal treatment, the fluorinated mixed oxides are obtained, with their surfaces having $MgO_{6-x}F_x$ species. Some of the microdomains of these species are enriched in oxygen, while others are enriched in fluorine. The memory effect was used to homogenize the distribution of oxygen and fluorine in $MgO_{6-x}F_x$ species. Solid-state ^{19}F and ^{27}Al NMR and the adsorption of nitromethane monitored by ^{13}C NMR showed that the fluorine incorporation into LDH leads to the formation of strong basic sites and a high density of aluminum with low coordination numbers.

AUTHOR INFORMATION

Corresponding Author

*E-mail: lima@iim.unam.mx. Phone: +52 (55) 5622 4640. Fax: +52 (55) 5616 1371.

Notes

The authors declare no competing financial interest.

ACKNOWLEDGMENTS

The authors would like to acknowledge CONACYT for Grant 128299 and PAPIIT-UNAM IN107110. We are grateful to A.Tejeda, M. Canseco, and E. Fregoso for their technical assistance.

REFERENCES

(1) *Layered Double Hydroxides: Present and Future*; Rives, V., Ed.; Nova Science Publishers, Inc.: New York, 2001.
(2) Occelli, M. L.; Olivier, J. P.; Auroux, A.; Kalwei, M.; Eckert., H. *Chem. Mater.* **2003**, *15*, 4231−4238.
(3) Hattori, H. *Chem. Rev.* **1995**, *95*, 537−550.
(4) Figueras, F. *Top. Catal.* **2004**, *29*, 189.
(5) Reinholdt, M. X.; Kirkpatrick, R. J. *Chem. Mater.* **2006**, *18*, 2567−2576.
(6) Gérardin, C.; Kostadinova, D.; Coq, B.; Tichit, D. *Chem. Mater.* **2008**, *20*, 2086−2094.
(7) In *Layered Double Hydroxides*; Duan, X., Evans, D. G., Eds.; Springer-Verlag: Berlin, 2006.
(8) Miyata, S. *Clays Clay Miner.* **1975**, *23*, 369.
(9) Beaudot, P.; De Roy, M. E.; Besse, J. *Chem. Mater.* **2004**, *16*, 935−945.
(10) Costantino, U.; Coletti, N.; Nocchetti, M. *Langmuir* **1999**, *15*, 4454−4460.
(11) Pfeiffer, H.; Lima, E.; Lara, V.; Valente, J. S. *Langmuir* **2010**, *26*, 4074−4079.
(12) Xu, Z. P.; Zeng, H. C. *Chem. Mater.* **2001**, *13*, 4564−4572.
(13) Stanimirova, T. S.; Vergilov, I.; Kirov, G.; Petrova, N. *J. Mater. Sci.* **1999**, *34*, 4153−4161.
(14) Martínez-Ortiz, M. J.; Lima, E.; Lara, V.; Méndez Vivar, J. *Langmuir* **2008**, *24*, 8904−8911.
(15) Hibino, T.; Tsunashima, A. *Chem. Mater.* **1998**, *10*, 4055−4061.
(16) Dávila, V.; Lima, E.; Bulbulian, S.; Bosch, P. *Microporous Mesoporous Mater.* **2008**, *107*, 240−246.
(17) Mackenzie, K. J.; Meinhald, R. H.; Sherriff, B. L.; Xu, Z. J. *J. Mater. Chem.* **1993**, *3*, 1263−1269.
(18) Wu, G.; Wang, X.; Wei, W.; Sun, Y. *Appl. Catal., A* **2010**, *377*, 107−113.
(19) Wu, G.; Wang, X.; Chen, B.; Li, J.; Zhao, N.; Wei, W.; Sun, Y. *Appl. Catal., A* **2007**, *329*, 106−111.
(20) Álvarez, M. G.; Chimentão, R. J.; Figueras, F.; Medina, F. *Appl. Clay Sci.* **2012**, *58*, 16−24.
(21) Hines, D. R.; Solin, S. A.; Costantino, U.; Nocchetti, M. *Phys. Rev. B* **2000**, *61*, 11348−11358.
(22) Hudlický, M. *Fluorine Chemistry for Organic Chemists*; Oxford University Press: Berlin, 2000.
(23) Chupas, P. J.; Corbin, D. R.; Rao, V. N. M.; Hanson, J. C.; Grey, C. P. *J. Phys. Chem. B* **2003**, *107*, 8327−8336.
(24) Murthy, J. K.; Gross, U.; Rüdiger, S.; Ünveren, E.; Kemnitz, E. *J. Fluorine Chem.* **2004**, *125*, 937−949.
(25) Body, M.; Silly, G.; Legein, C.; Buzaré, Y. *Inorg. Chem.* **2004**, *43*, 2474−2485.
(26) Hefter, G.; Bodor, A.; Tóth, I. *Aust. J. Chem.* **2000**, *53*, 625−626.
(27) Akdeniz, Z.; Tosi, M. P. *Phys. Chem. Liq.* **1990**, *21*, 127−136.
(28) Kon'shin, V. V.; Chernyshov, B. N.; Ippolitov, E. G. *Dokl. Akad. Nauk SSSR* **1984**, *278*, 370.
(29) Castellan, G. W. *Physical Chemistry*, 3rd ed.; Addison-Wesley Publishing Co.: Boston, MA, 1964.
(30) Scholz, G.; Stosiek, C.; Noack, J.; Kemnitz, E. *J. Fluorine Chem.* **2011**, *132*, 1079−1085.
(31) Prescott, H. A.; Li, Z.-J.; Kemnitz, E.; Deutsch, J.; Lieske, H. *J. Mater. Chem.* **2005**, *15*, 4616−4628.
(32) Dambournet, D.; Demourgues, A.; Martineau, C.; Pechev, S.; Durand, E.; Lhoste, J.; Majimel, J.; Vimont, A.; Lavalley, J.-C.; Daturi, M.; Legein, C.; Buzaré, J.-Y.; Fayon, F.; Tressaud, A. *Chem. Mater.* **2008**, *20*, 1459−1469.
(33) Lippmaa, E.; Samoson, A. *J. Am. Chem. Soc.* **1986**, *108*, 1730−1735.
(34) Samoson, A.; Lippmaa, E.; Engelhardt, G.; Lohse, U.; Jerschkewitz, H. J. *Chem. Phys. Lett.* **1987**, *134*, 589−592.
(35) Coster, D.; Blumenfeld, A. L.; Fripiat, J. J. *J. Phys. Chem.* **1994**, *98*, 6201−6211.
(36) Bokhimi, X.; Lima, E.; Valente, J. *J. Phys. Chem. B* **2005**, *109*, 22222−22227.
(37) Gazzano, M.; Kagunya, W.; Matteuzzi, D.; Vaccari, A. *J. Phys. Chem. B* **1997**, *101*, 4514−4519.
(38) Sampieri, A.; Lima, E. *Langmuir* **2009**, *25*, 3634−3639.
(39) Lavalley, J. C. *Catal. Today* **1996**, *27*, 377−401.
(40) Sing, K. S. W.; Everett, D. H.; Haul, R. A.; Moscou, L.; Pieorotti, R. A.; Rouquerol, J.; Siemienniewska, T. *Pure Appl. Chem.* **1985**, *57*, 603−619.
(41) Veldurthy, B.; Clacens, J.-M.; Figueras, F. *J. Catal.* **2005**, *229*, 237−242.
(42) Kheir, A. A.; Haw, J. F. *J. Am. Chem. Soc.* **1994**, *116*, 817−818.

(43) Lima, E.; de Ménorval, L.-C.; Tichit, D.; Laspéras, M.; Graffin, P.; Fajula, F. *J. Phys. Chem. B* **2003**, *107*, 4070−4073.
(44) Lima, E.; Laspéras, M.; de Ménorval, L.-C.; Tichit, D.; Fajula, F. *J. Catal.* **2004**, *223*, 28−35.